An Investigation of the Conformational and Self-Aggregational Processes of Histones Using ^1H and ^{13}C Nuclear Magnetic Resonance†

D. M. J. Lilley, O. W. Howarth, V. M. Clark,* J. F. Pardon, and B. M. Richards

ABSTRACT: Histone self-aggregation processes have been studied by ^{13}C and ^1H nuclear magnetic resonance (NMR) as a function of ionic strength and protein concentration. This has led to a model involving apolar aggregation between structured regions of these molecules. This analysis supports the validity of the acquisition of conformational data on histones by the simulation of ^{13}C NMR spectra at high concentration. Solution conformations for histones F2B and F3 are presented.

In the chromatin of eukaryotic organisms DNA is complexed with five types of histones (Johns, 1967a,b) which are thought to be responsible for the contraction of the nucleic acid into a folded or coiled conformation. X-Ray diffraction studies of isolated chromatin have revealed (Luzzati and Nicolaieff, 1963; Richards and Pardon, 1970) a repeat distance of 110 Å, which has led to the super-coil model (Pardon and Wilkins, 1972), and recent evidence from many techniques has led to the suggestion of a subunit construction for chromatin (Kornberg, 1974). An integral part of the postulated subunit structure is specific heterologous interaction between the histones and there have been several such complexes reported (D'Anna and Isenberg, 1973; Kelley, 1973; Clark et al., 1974; Kornberg and Thomas, 1974). In order to gain some insight into the nature of this interaction, and ultimately the means by which super-coiling is induced in the DNA, it is first necessary to have a knowledge of the solution conformation of the individual histones.

Optical methods have been applied extensively to solutions of histones (Bradbury et al., 1967; Li et al., 1972; D'Anna and Isenberg, 1974a,b), both individually and as mixtures, but while they can provide information on helical content they cannot indicate the distribution of secondary structure with respect to the primary structure of these molecules. Nuclear magnetic resonance (NMR) is capable of yielding more detailed information. Boublik et al. (1970) and Bradbury and Rattle (1972) have used ^1H NMR in a series of studies of histone solution conformation, concluding that histones in pure water are entirely in the random-coil state and that regular secondary structure is only induced on raising the ionic strength. In a previous paper (Clark et al., 1974) we have shown that ^{13}C NMR may be used to study histone conformation. The results indicated that histones $F2A_1$ and $F2A_2$ in pure water both contain considerable secondary structure which is located away from the N-terminus. An important difference between the experimental techniques for the ^{13}C and ^1H studies was the concentration of histone solutions examined. The low natural abundance and sensitivity of ^{13}C had required us to work with solutions which were ten times the concentration used in the ^1H NMR work (i.e., 100 mg/ml and 10 mg/ml, respectively). The physiological significance of this is not easy to assess, for the concentration of histone in either the nuclear volume or in chromatin is not available, but it is likely that our more concentrated samples are a better representation of the in vivo state than the lower concentrations used by other workers.

Histones are known to aggregate, even at protein concentrations below 1 mg/ml. It is likely that considerable aggregation occurs at concentrations of 100 mg/ml. To investigate this aggregation we have studied both ^1H and ^{13}C spectra over a range of histone concentrations. It has been possible both to determine which regions of the histones are involved in homologous interactions and also to show that the aggregation process does not affect the secondary structure of the histones. The original ^{13}C studies of histones $F2A_1$ and $F2A_2$ (Clark et al., 1974) have been extended and similar studies made with histones F2B and F3.

Experimental Section

Histones were extracted from calf thymus using the methods of Johns (1967a,b). In the cases of $F2A_1$ and $F2A_2$, three ethanol washes were performed before the final acetone wash (Clark et al., 1974). Spectra were recorded as soon as possible after preparation, all samples being stored at 0°C under acetone and the acetone removed under vacuum for 24 hr immediately prior to use. The purity of all histone fractions was checked by polyacrylamide gel electrophoresis (Panyim and Chalkley, 1969). All histone solutions used for NMR experiments were homogeneous.

^{13}C NMR at 22.63 MHz and Computer Simulation of Spectra Obtained at 100 mg/ml. This has been described previously (Clark et al., 1974). Proton noise-decoupled ^{13}C NMR spectra were recorded at 22.63 MHz on a Bruker WH-90 instrument. Spectra were obtained in 1-ml sample volumes at protein concentrations of 100 mg/ml, dissolved in glass distilled water containing 30% deuterium oxide.

^{13}C NMR at 45.26 MHz. Proton noise-decoupled ^{13}C NMR spectra at natural abundance were recorded at 45.26 MHz in the Fourier transform mode on a Bruker WH-180 wide-bore spectrometer. This instrument was equipped with a Bruker superconducting magnet, a probe of internal di-

† From the Department of Molecular Sciences, University of Warwick, Coventry, CV4 7AL, England (D.M.J.L., O.W.H., V.M.C.), and Searle Research Laboratories, High Wycombe, HP12 4HL, England (J.F.P., B.M.R.). *Received March 7, 1975.* Financial support (for D.M.J.L.) from Twyford Laboratories is gratefully acknowledged.

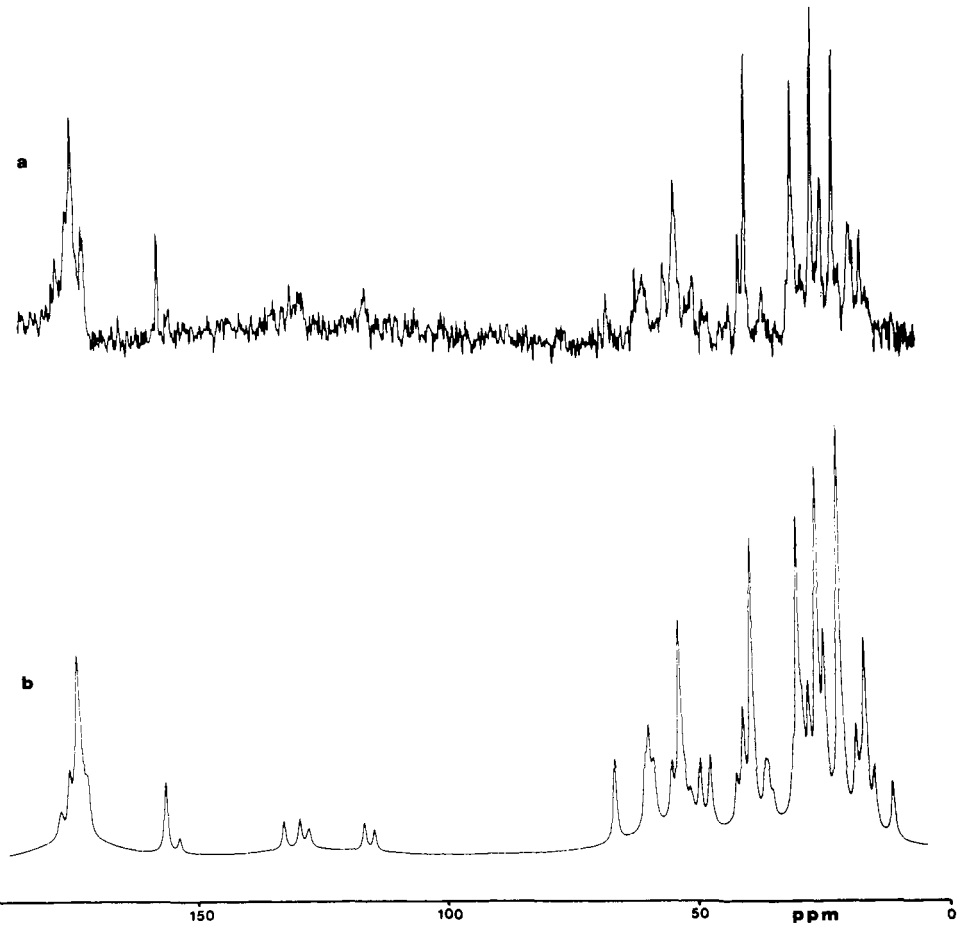

FIGURE 1: ^{13}C NMR spectrum and simulation for histone F2B: (a) spectrum of 100 mg/ml solution of F2B in H_2O–30% D_2O; 3×10^5 accumulations; shifts in parts per million relative to Me_4Si; (b) simulation of (a) assuming free motion in residues 1–35, 49–54, and 79–90 and structure in residues 36–48, 55–78, and 91–125.

ameter 30 mm, and a quadrature detection system. Spinning sample tubes (25 mm diameter) were used at probe temperatures 280–290 K. Sweep width and frequency offset were set to give spectra equivalent to those recorded on the Bruker WH-90; a 60° pulse (30 μsec) was used with a 0.4-sec recycle time. Data were collected in 8192 points in the time domain (i.e., 4096 points for the real free induction decay) and 4–6 × 10^4 pulses were recorded for each spectrum. Histone samples were dissolved at 10 mg/ml in 30 ml of distilled water, containing 17% D_2O to provide a field lock. In some samples sodium chloride was added directly to the histone solution in the NMR tube to give the desired concentration.

Computer Simulation of ^{13}C NMR Spectra Obtained at 10 mg/ml. This program was constructed using basically the same approach as that for the spectra at higher concentrations (Clark et al., 1974). The primary sequence of the protein was divided into regions of two types, those considered to be involved in secondary structure and those likely to be in random-coil and capable of free movement. Two stick maps of resonances were then calculated using published data for ^{13}C shifts in amino acids and proteins. The peak heights thus obtained were scaled to allow for nuclear Overhauser enhancement (NOE) resulting from proton noise decoupling. For the carbon atoms of the "free" regions, this scaling factor was set at a maximum for any carbon atom possessing a directly bonded proton, but for the "structured" regions full NOE is only allowed for carbon atoms further removed from the backbone than the β carbon. The free stick map was fitted to a Lorentzian line shape of given width but the structured resonances were adjusted to include line-broadening effects. Thus, peak heights were reduced and widths increased by different factors determined by the proximity of the appropriate ^{13}C atom to the backbone and the number of directly bonded protons.

^1H spectra were recorded at 90 MHz on a Bruker WH-90 Fourier transform instrument. The height of the HDO peak was attenuated by irradiation in a gated mode. Spinning sample tubes (5 mm) were used, at probe temperatures of 280–290 K. Histone samples were dissolved in 99.8% D_2O (Fluorochem Ltd.) containing the desired concentration of NaCl.

Results and Discussion

22.63-MHz ^{13}C Spectra of F2B and F3. Proton-decoupled ^{13}C NMR spectra for these histones at a concentration of 100 mg/ml are shown in Figures 1 and 2. These spectra show similarities to those of $F2A_1$ and $F2A_2$ (Clark et al., 1974) but are quite clearly distinguishable. A common feature in all these spectra is the superimposition of a number of comparatively sharp resonances onto a rather broader background. This is consistent with the molecules containing some regions which are structured and others which are capable of comparatively free motion.

Using the simulation program described previously (Clark et al., 1974) close agreement has been obtained between simulated and observed spectra (Figures 1 and 2). For F2B the best simulation was obtained where residues

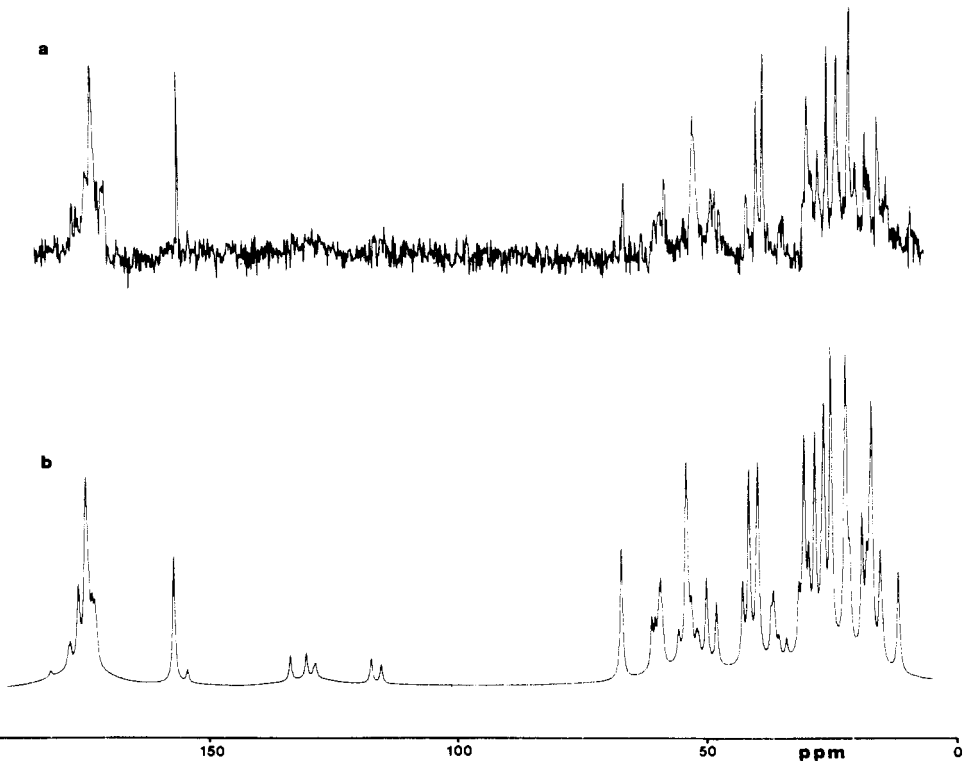

FIGURE 2: ^{13}C NMR spectrum and simulation for histone F3: (a) spectrum of 100 mg/ml solution of F3 in H_2O–30% D_2O; 3.1×10^5 accumulations; (b) simulation of (a) assuming free motion in residues 1–20, 27–46, and 106–135 and structure in residues 21–26 and 47–105.

1–35, 49–54, and 79–90 were allowed freedom of motion, the rest of the molecule being structured (Figure 1). The simulation procedure was estimated to be sensitive to changes in boundary position of at most two residues on either side. For F3 the best simulation was obtained assuming free motion in the residues 1–20, 27–46, and 106–135, and two structured regions at 21–26 and 47–105 (Figure 2). It is to be noted that the regions of structure in both histones derived by this method are in close agreement with those predicted (Pardon and Richards, 1973) for the presence of α helix using the rules of Prothero (1966) and Schiffer and Edmundson (1967).

A common feature of all the histone conformations determined by means of ^{13}C NMR is a freely mobile N-terminal peptide containing a large number of basic residues, which accords with the view generally held that it is this region which is involved in binding to DNA in chromatin.

In contrast with the behavior exhibited by histone $F2A_1$, raising the ionic strength of 100 mg/ml solutions of F2B and F3 produced a comparatively slight overall reduction in signal-to-noise ratio. Figure 3 shows spectra of F2B and F3 at 0.4 and 0.6 *M* sodium chloride, respectively. Some reduction in signal-to-noise is evident but the spectra are qualitatively essentially the same as the zero ionic strength solutions. It is apparent that histones $F2A_2$, F2B, and F3 are less susceptible to salt induced aggregation than is $F2A_1$.

90-MHz ^1H Spectra of $F2A_1$, $F2A_2$, F2B, and F3. (a) Histone $F2A_2$. Proton NMR spectra of histone $F2A_2$ at 100, 30, and 10 mg/ml are shown in Figure 4. While the 100 and 30 mg/ml spectra are quite similar, at 10 mg/ml there are changes. An assignment for some of the resonances (McDonald and Phillips, 1969) is shown on the lower concentration spectrum. The regions showing concentration-dependent effects are the methyl resonances of valine, leucine, and isoleucine, occurring at the high-field end of the spectrum, and the aromatic region, downfield from the HDO peak, all of which show a decrease in apparent intensity with increasing histone concentration. Phenylalanine, tyrosine, valine, leucine, and isoleucine are all residues of distinctly hydrophobic character and hence it seems reasonable that the spectral change observed may be ascribed to processes involving apolar aggregation. While a simple helix–coil transition would be expected to affect the correlation times of backbone and β-CH protons and, hence, their resonance line widths, many side-chain protons should still be capable of rapid isotropic motion and thus produce narrow resonances. However, aggregation between the hydrophobic side chains of regions which are already involved in secondary structure would be predicted to lead to just the changes in the spectra which have been observed. It can also be seen that of the aromatics, tyrosine shows the major signal loss from broadening effects.

Simulation of the ^{13}C NMR spectra of $F2A_2$ at 100 mg/ml indicated that the primary sequence could be divided into structured regions between residues 40–70 and 96–116, the rest of the molecule being freely mobile. The structured regions contain a high proportion of valine, leucine, and isoleucine and also tyrosine as the only aromatic residue. Furthermore, if a model of the 40–70 regions is built assuming 3.6 residues per turn, then it is seen that Tyr-50 and Tyr-57 lie on the same side of the helix and that Tyr-39, while being considered formally as lying in the free region, is also coaligned. Hence, hydrophobic aggregation of $F2A_2$ molecules by the central 40–70 region, either alone or in concert with the 96–116 region, is entirely consistent with the observed spectral changes.

The effects of raising the ionic strength may also be rationalized within the above framework. Figure 5 shows the effect of various concentrations of sodium chloride upon the ^1H spectrum of $F2A_2$ at 10 mg/ml protein. At the lowest

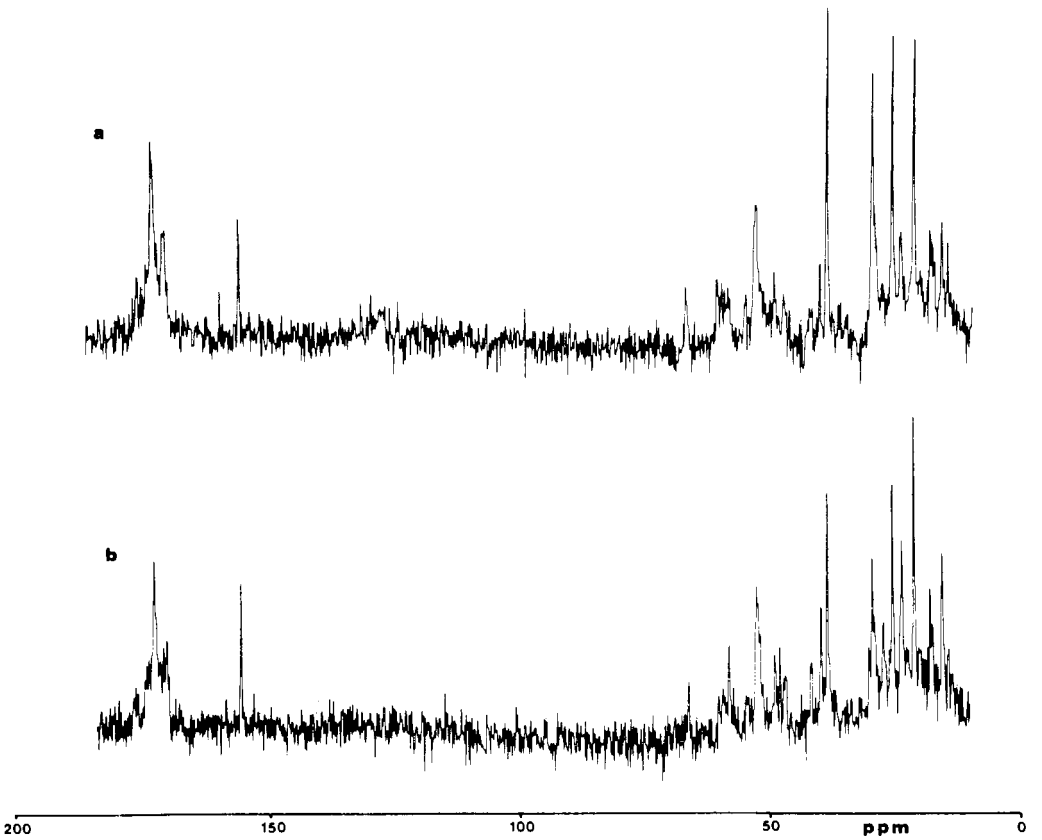

FIGURE 3: (a) ^{13}C NMR spectrum of 100 mg/ml solution of F2B in 0.4 *M* NaCl in H_2O–30% D_2O; 2.7×10^5 accumulations; (b) ^{13}C NMR spectrum of 100 mg/ml solution of F3 in 0.6 *M* NaCl in H_2O–30% D_2O; 2.3×10^5 accumulations.

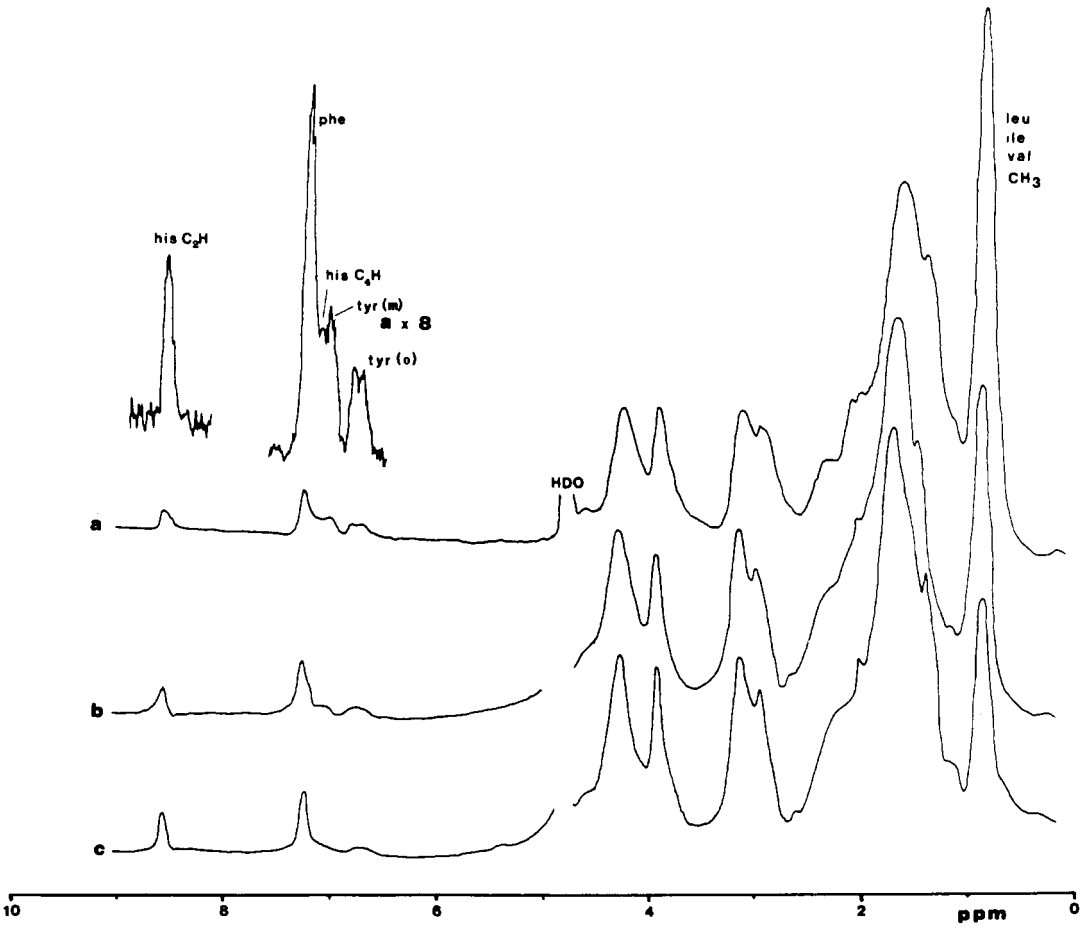

FIGURE 4: ^1H NMR spectra of solution of histone $F2A_2$ in D_2O: (a) 10 mg/ml, some resonances have been assigned on this spectrum; (b) 30 mg/ml; (c) 100 mg/ml.

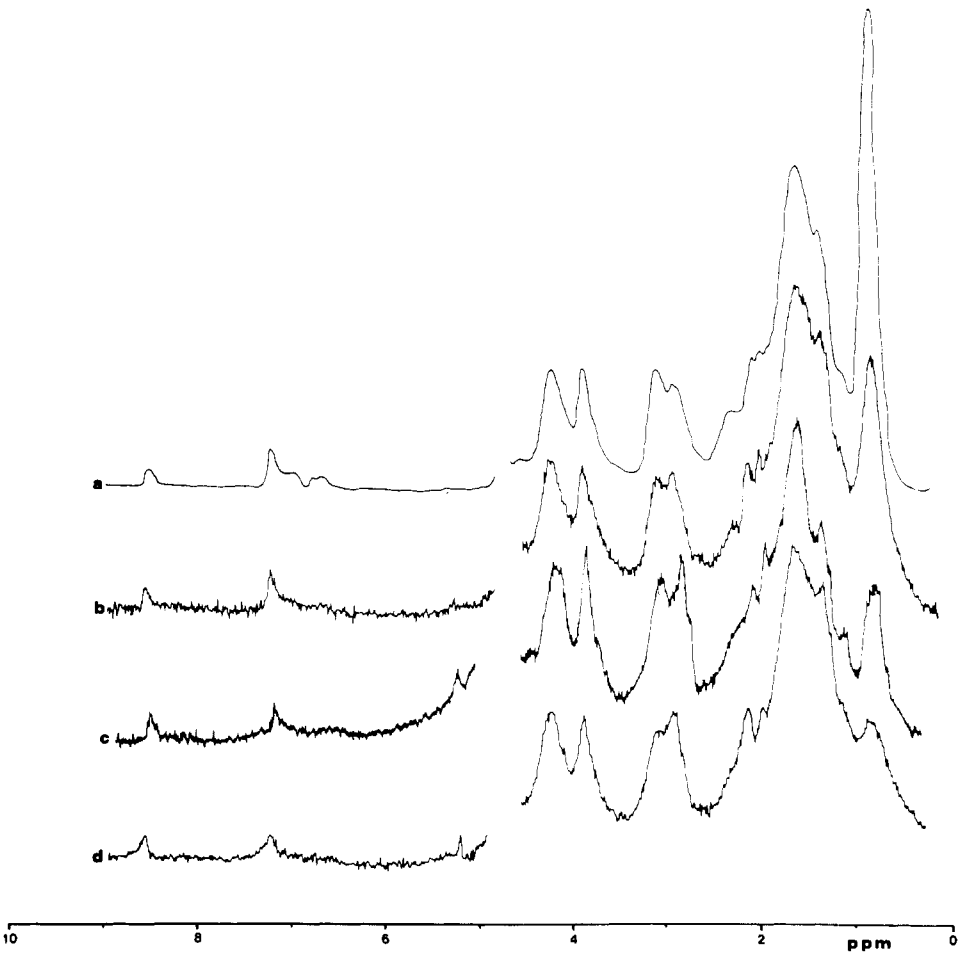

FIGURE 5: ^{1}H NMR spectra of 10 mg/ml solutions of histone $F2A_2$ in: (a) pure D_2O; (b) 0.1 *M* NaCl in D_2O; (c) 0.6 *M* NaCl in D_2O; (d) 1.0 *M* NaCl in D_2O.

sodium chloride concentration, the spectrum is closely similar to that recorded at 100 mg/ml in the absence of any salt. The methyl region of the spectrum has been considerably reduced in apparent intensity. Tyrosine is the most affected aromatic residue, being almost indistinguishable from noise at 0.1 *M* sodium chloride. As the sodium chloride concentration is raised from 0.1 to 0.6 *M*, the methyl region continues to decrease in intensity, but the phenylalanine and histidine intensities are not reduced further. At 1 *M* sodium chloride the methyl region has suffered extensive broadening and the histidine has undergone some intensity loss. The similarity between the effects of protein concentration and those of raising the ionic strength of the histone solution suggest that a common mechanism is involved whereby the addition of sodium chloride to a solution of $F2A_2$ induces aggregation between the structured hydrophobic region(s) of the molecule. As for the protein concentration effects this aggregation might occur with both structured regions or just the central 40–70 region. As the ionic strength is raised beyond 0.1 *M* the spectral changes indicate that this binding becomes tighter. That the major effect is on the methyl resonances indicates that the aromatic (tyrosine) residues are most involved in the apolar aggregation, even at the lower salt concentration, but that a further increase in ionic strength leads to a packing down process, further immobilizing the methyl groups of the hydrophobic aliphatic residues. The loss of histidine intensity at the highest ionic strength may reflect a stronger binding of the second structured region, i.e. that between residues 83 and 116, thereby affecting the mobility of the formally free central region, residues 71–82, which includes the His-82 residue.

(b) Histones F2B and F3. ^{1}H spectra of F2B and F3 at 100 and 10 mg/ml are shown in Figures 6 and 7. As for the $F2A_2$ spectra there are marked changes in the region corresponding to hydrophobic residues, in particular the methyl region being considerably reduced in apparent intensity. Of the aromatic residues, the predominant reduction in both histones is in the phenylalanine peaks, suggesting that in the apolar aggregation the major aromatic participant is phenylalanine. In our predicted conformation for F3, the longer structured region, i.e. that between residues 47 and 105, contains four phenylalanine and two tyrosine residues. Thus, aggregation between these regions of two or more F3 molecules would be expected to produce a major effect on the phenylalanine resonances and a lesser effect on the tyrosine peaks. Indeed, closer examination of Figure 7 shows that a reduction in apparent intensity of the tyrosine resonances has occurred, the change being about half the magnitude of the phenylalanine reduction. The ^{13}C spectrum of F2B indicated the presence of three structured regions of the molecule. All contain a high proportion of hydrophobic residues but the regions differ in their aromatic residue content. The region between residues 35 and 48 contains three tyrosine residues, that between 55 and 78 contains two phenylalanine, and that from 91 to 125 contains one tyrosine and one histidine residue. As well as the major phenylalanine reduction in the spectra, some loss of intensity is also

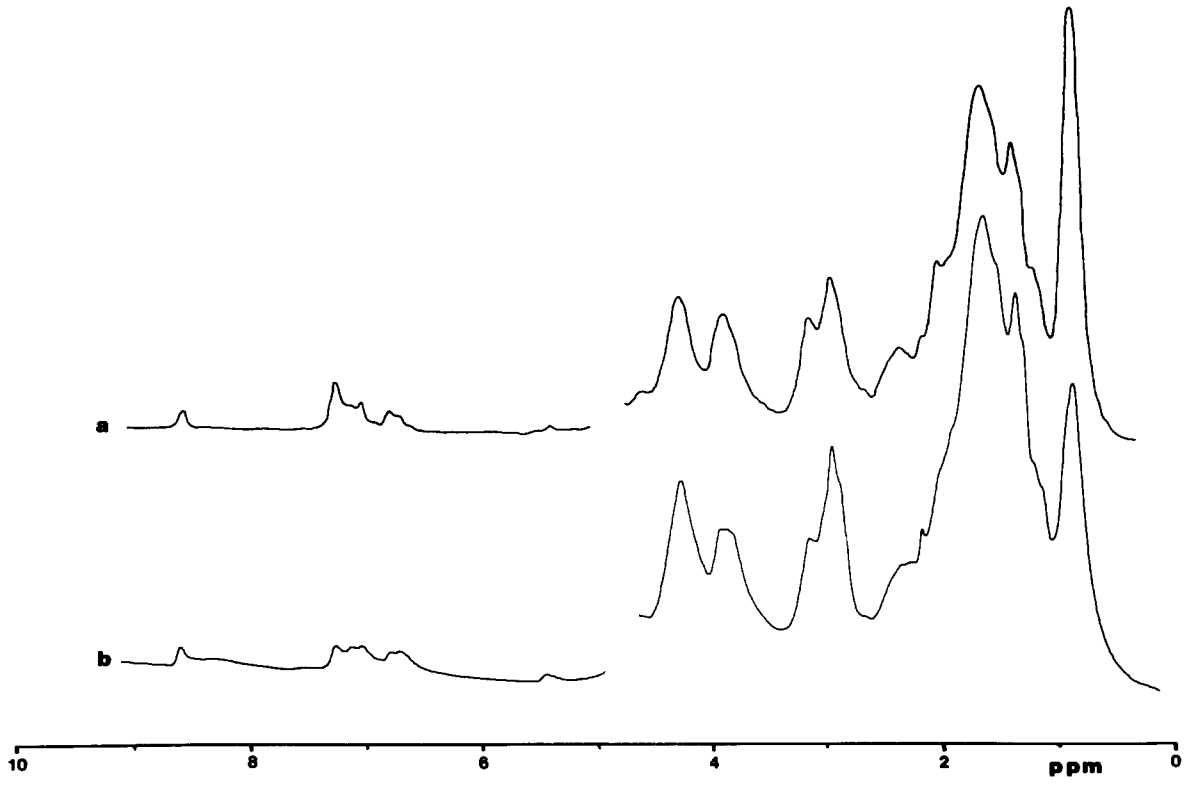

FIGURE 6: ^{1}H NMR spectra of solutions of histone F2B in D_2O: (a) 10 mg/ml; (b) 100 mg/ml.

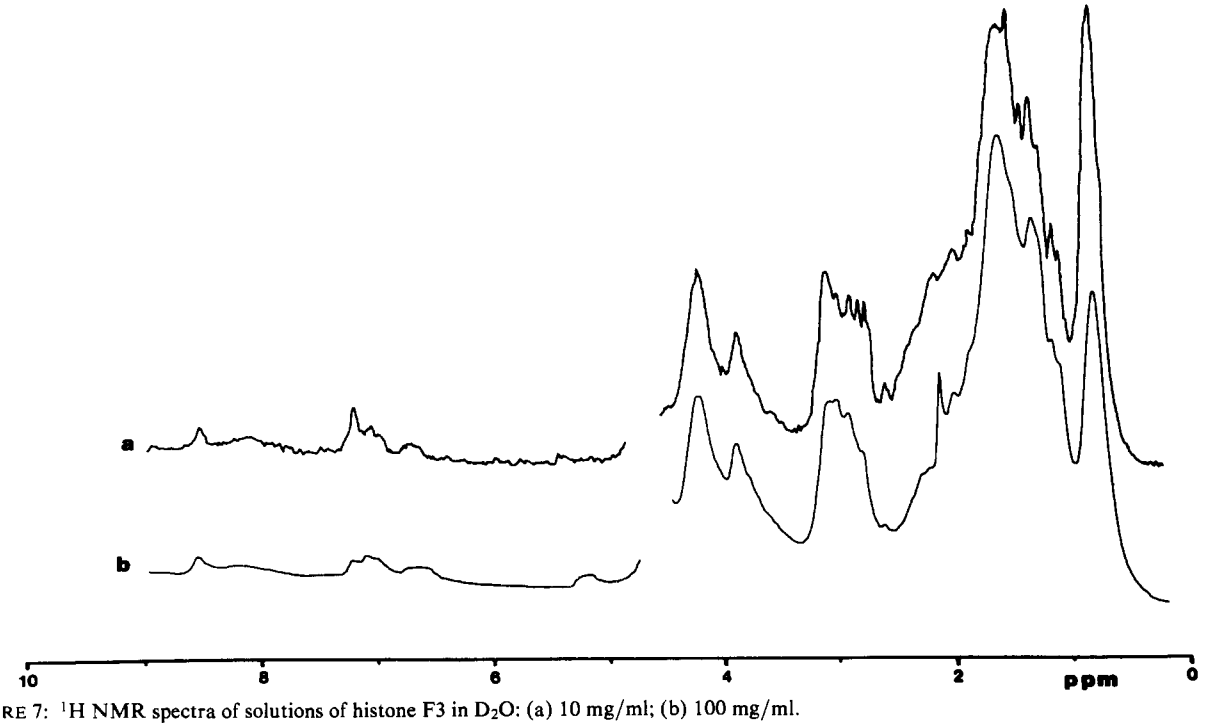

FIGURE 7: ^{1}H NMR spectra of solutions of histone F3 in D_2O: (a) 10 mg/ml; (b) 100 mg/ml.

evident in the tyrosine resonances, though again this effect is smaller than the phenylalanine reduction. Thus, it would appear that while all the structured regions are showing some aggregation, the most important is the central region, containing residues 55–78.

Spectral variations with ionic strength are similar to those for $F2A_2$ and again the similarity with the protein concentration effects is marked. The methyl region shows the same continuous reduction in intensity as the ionic strength is increased but the aromatic residue most affected is phenylalanine; again this effect is particularly evident between 0 and 0.1 *M* sodium chloride. This result is entirely consistent with the above analysis for $F2A_2$ and with the observed protein concentration dependence of the spectra, thus reinforcing the conclusion that the central 55–78 region of structure is the most important in the aggregation process. However, it is evident that the other structured regions suffer some degree of aggregation as evidenced by a loss of intensity of tyrosine and histidine at higher salt concentrations.

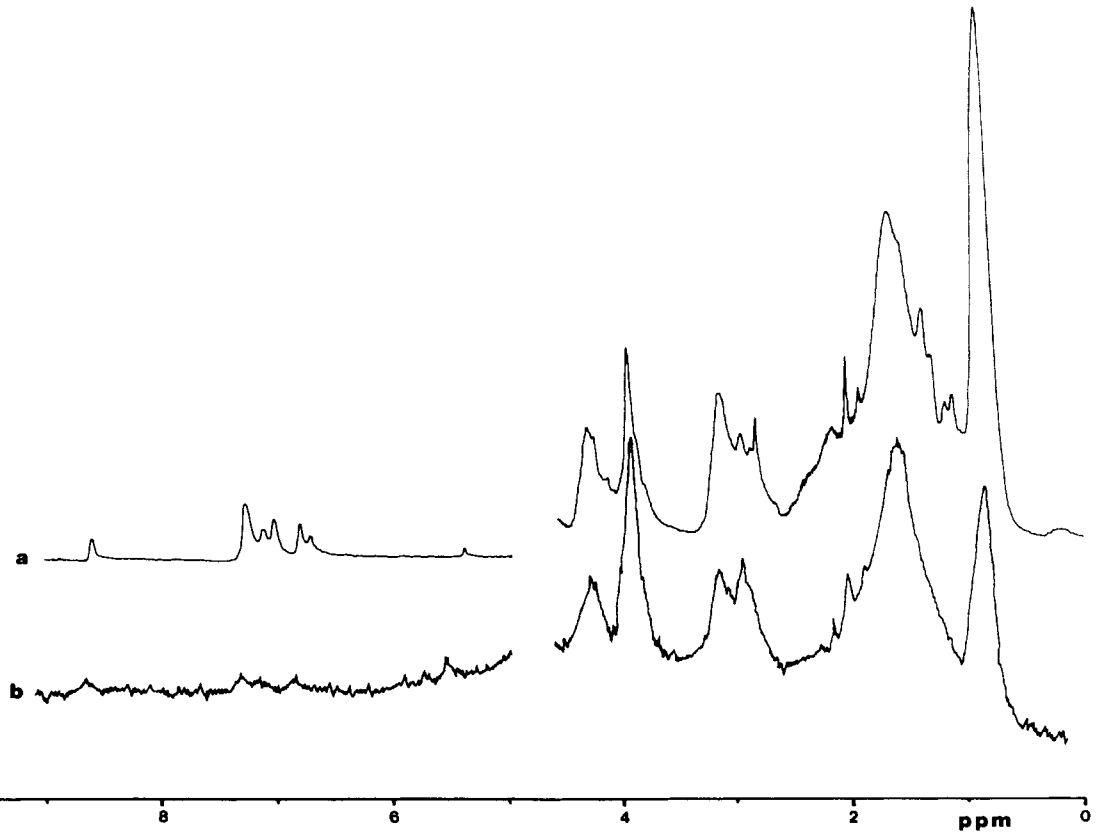

FIGURE 8: ^{1}H NMR spectra of solutions of histone F2A$_1$ in D_2O: (a) 10 mg/ml; (b) 66 mg/ml.

(c) Histone F2A$_1$. ^{1}H spectra for F2A$_1$ at 66 and 10 mg/ml are shown in Figure 8. Together with the methyl region there is a large overall reduction in intensity of all the aromatics. In contrast to the previous three histones there are no differential effects between the reduction in intensities shown by the three aromatic types. The conformation of F2A$_1$ which was derived from analysis of ^{13}C NMR spectra (Clark et al., 1974) indicated that this histone is more structured than the other three, being entirely immobilized from residue 26 to the C terminus. This region contains many hydrophobic residues and all three types of aromatic residues, and hence aggregation of this region would be expected to affect the resonances of all the aromatic residues, as observed.

If the ionic strength is increased at 10 mg/ml protein the spectra show losses of apparent intensity in the methyl region and in all the aromatic types. This is again consistent with our proposed conformation for F2A$_1$ and with the salt-induced aggregation mechanism. That this is a reversible process has been demonstrated by examination of the ^{1}H spectrum of a solution of F2A$_2$ in D_2O which has been dialyzed from 0.5 *M* sodium chloride against 100 vol of D_2O overnight; both the methyl and the aromatic residues regain the relative intensity observed at zero ionic strength before the addition of salt.

^{13}C Spectra at 10 mg/ml of F2A$_1$ and F2A$_2$. The ^{13}C NMR spectrum of a 10 mg/ml solution of histone F2A$_1$ is shown in Figure 9. Comparison with that obtained at 100 mg/ml (Clark et al., 1974) shows an essential similarity but the two spectra are not identical. The general line width is narrower in the former spectrum, this being due in part to the higher field used for the lower concentration, and the two spectra show several differences in the intensities of some resonances. In particular, the aromatic region, 100–150 ppm, shows the greatest increase in intensity and both the methyl region, upfield from 20 ppm, and the α-carbon region, 50–70 ppm, are clearly increased. Furthermore, there are differences in the relative intensities of lines in the general aliphatic region, 20–50 ppm. The best simulation of this spectrum, based on the conformation obtained from the ^{13}C NMR spectrum at 100 mg/ml and using the method outlined in the Experimental Section, is also shown in Figure 9, together with that obtained using the same procedure but with the assumption of an entirely unstructured molecule. Bearing in mind the relative simplicity of this approach, the agreement between the actual F2A$_1$ spectrum and the simulation based on the structured conformation is good.

^{13}C NMR spectra and simulations for a 10 mg/ml solution of F2A$_2$ are shown in Figure 10. Comparison with the spectrum at 100 mg/ml (Clark et al., 1974) shows fewer differences, but the overall pattern of increased intensity in aromatic, methyl, and α-carbon regions is observed. The general line width is greater than in the F2A$_1$ spectrum. Agreement between the F2A$_2$ spectrum and its simulation based upon the structure derived from ^{13}C NMR at 100 mg/ml is again good.

Most of the discrepancies between actual and simulated spectra may be ascribed to the inherent simplicity of this approach. Thus, a consistent error in our simulations is the relatively low intensity of the peak at 40.5 ppm, which has been assigned to arginine (δ). The observed line widths are composed of the natural carbon line widths plus the effects of small chemical shifts between different residues of any given type due to slight variations of environment. This latter effect would be expected to be least pronounced near the end of a long side chain and so the apparent line width of a resonance such as arginine δ should be narrower, with a cor-

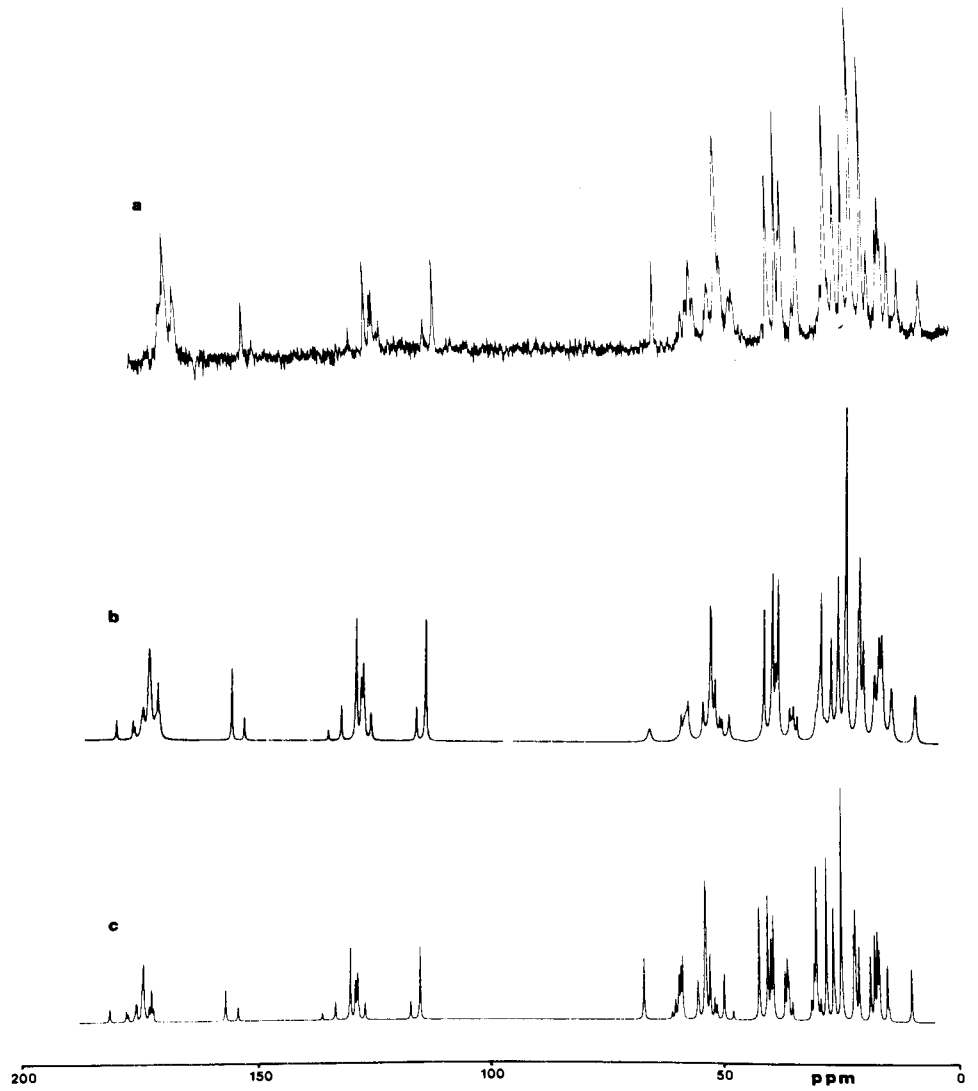

FIGURE 9: ^{13}C NMR spectrum and simulations for histone $F2A_1$: (a) spectrum of 10 mg/ml solution of $F2A_1$ in H_2O–16% D_2O; 4×10^4 accumulations; (b) simulation of (a) assuming free motion in residues 1–26 and structure in residues 27–102; (c) simulation of (a) assuming totally random coil molecule.

responding increase in peak height. Another discrepancy consistently observed has been in the region 35–37 ppm, thought to result from slight errors in our original shift data.

Nevertheless, with these reservations in mind, it is important to appreciate that the agreement between simulated and observed spectra has only been possible with the assumption of a model in which the molecules contain regions of secondary structure. Such regions would be predicted to result in substantial reduction of rapid isotropic motions in all backbone and β-carbon atoms, whereas in a random coiled molecule much smaller effects would be expected. In the simulation of $F2A_1$ a basic line width of 5 Hz has been used and 10 Hz for the $F2A_2$ simulation. The difference in line widths may result from the greater molecular weight of the $F2A_2$ molecule.

Regions of these histones containing secondary structure might be expected to be subject to further folding—the tertiary structure thus producing an overall globular conformation. Since no appreciable side-chain immobilization has been detected by the simulation method it is concluded that if tertiary structure exists, helix–helix contact must be at a minimum.

Figure 11 shows the effects of increased salt concentrations on the spectrum of $F2A_1$. Comparisons of this with the ^{13}C NMR spectrum obtained from 100 mg/ml solutions at zero ionic strength (Clark et al., 1974) show remarkable resemblances. Similar agreement is evident between the analogous spectra for histone $F2A_2$. Thus, it would appear that as judged by the ^{13}C NMR spectra of these histones, the effects of increased ionic strength and those of increased protein concentration are very similar, and that, therefore, a common mechanism is involved. These results and those from the ionic strength and protein concentration studies by ^1H NMR are completely consistent.

General Discussion

^{13}C studies of helix–coil transitions in polypeptides (Allerhand and Oldfield, 1973) have indicated that there is little change in side-chain relaxation times or NOE between the two forms. Hence, it would seem that in 100 mg/ml histone solutions there is an additional process providing a restraint on the motion of the entire side chain. Aggregation between side chains of distinct histone molecules could produce such an overall immobilization. The simulations are not very sensitive to the value for the broadening factor used, but 20 appears to be of the right order for the "structured" regions.

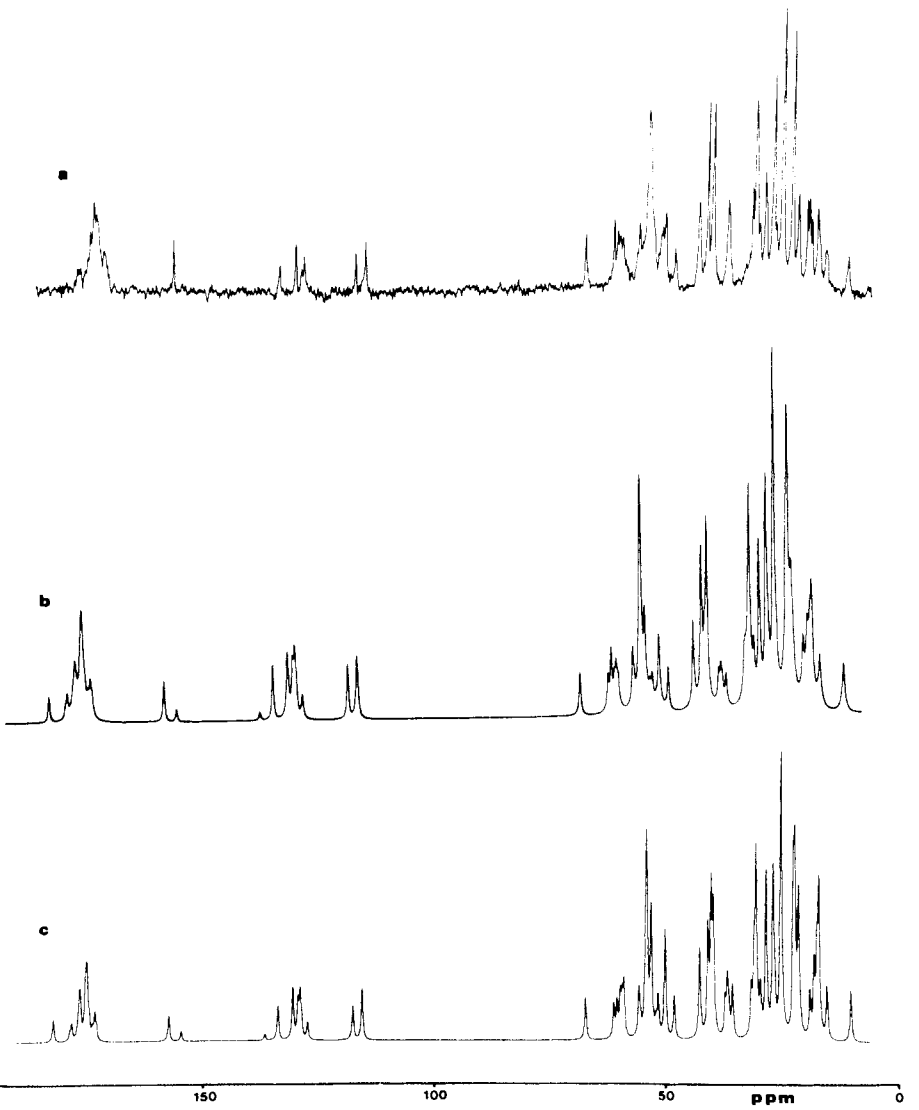

FIGURE 10: ^{13}C NMR spectrum and simulations for histone $F2A_2$: (a) spectrum of 10 mg/ml solution of $F2A_2$ in H_2O–16% D_2O; 4×10^4 accumulations; (b) simulation of (a) assuming free motion in residues 1–39, 71–83, and 117–129 and structure in residues 40–70 and 84–116; (c) simulation of (a) assuming totally random coil molecule.

Allerhand has shown (Doddrell et al., 1972) that ^{13}C relaxation in macromolecules is dominated by dipolar interaction with directly bound protons, if such exist. Thus, the transverse relaxation times, which are inversely proportional to line widths, will be given by:

$$\frac{1}{T_2} = \frac{N\gamma_C^2\gamma_H^2\hbar^2}{10r_{CH}^6} f(\tau_C) = \pi\Delta\nu \qquad (1)$$

for a CH decoupled system, where N is the number of directly bonded protons, γ_C and γ_H are the magnetogyric ratios of carbon and hydrogen, respectively, $\hbar$ is Planck's constant divided by 2π, r_{CH} is the length of the C–H vector, $\Delta\nu$ is the line width in hertz, and $f(\tau_C)$ is a function of the rotational correlation time (τ_C) given by:

$$f(\tau_C) = 2\tau_C + \frac{0.5\tau_C}{1 + (\omega_C - \omega_H)^2\tau_C^2} + \frac{1.5\tau_C}{1 + \omega_C^2\tau_C^2} + \frac{3\tau_C}{\omega_H^2\tau_C^2} + \frac{3\tau_C}{1 + (\omega_C + \omega_H)^2\tau_C^2} \qquad (2)$$

where ω_C and ω_H are the resonance frequencies of carbon and hydrogen, respectively, 1.49×10^8 rad sec^{-1} and 6.6×10^8 rad sec^{-1} at a field of 2.11 T. For any given carbon atom

$$\Delta\nu \propto f(\tau_C) \qquad (3)$$

and making the assumption that an unhindered side chain would have a correlation time of the order of 10^{-10} sec, whereas the overall tumbling time for a small protein is generally about 10^{-8} sec, substitution into eq 2 and 3 shows that:

$$\frac{\Delta\nu(\tau_C = 10^{-8})}{\Delta\nu(\tau_C = 10^{-10})} = 28$$

In view of the uncertainties in the actual correlation times involved, the agreement between the calculated factor and that necessary to obtain a good simulation is indicative that the order of magnitude in the change of mobility is correct. Thus, it does appear that in 100 mg/ml histone solutions aggregation is sufficiently extensive to immobilize completely the entire side chain.

In order to simulate the spectra from 10 mg/ml histone solutions, it was necessary to broaden the methylene carbons at positions γ and beyond by a factor of 2.5 for the

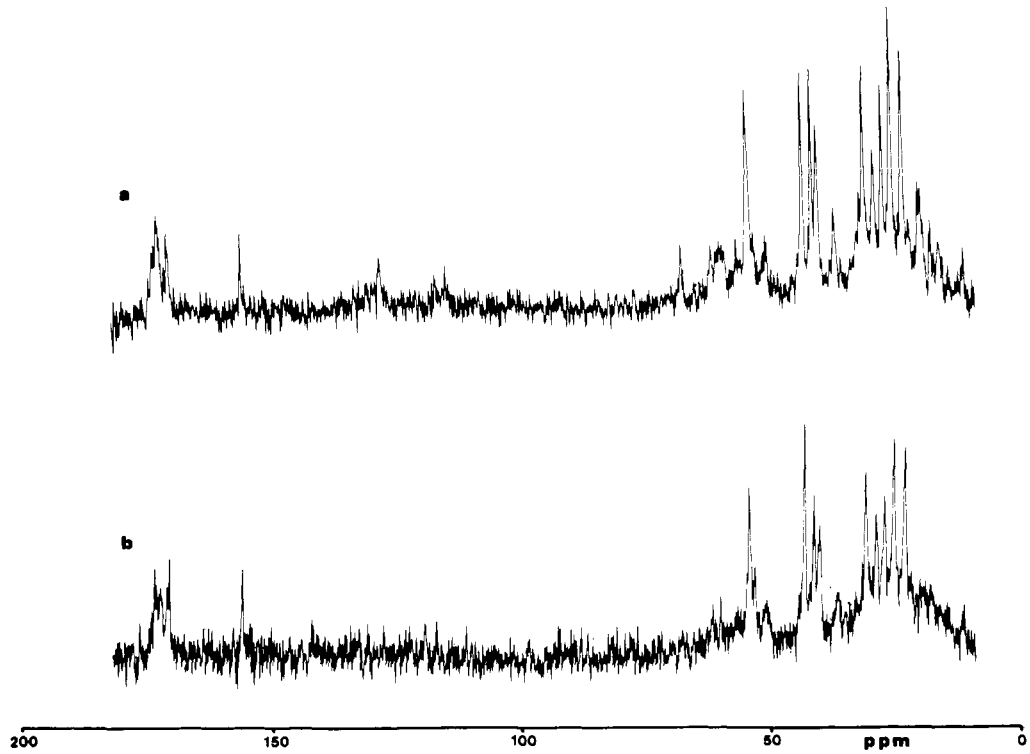

FIGURE 11: ^{13}C NMR spectra of 10 mg/ml solutions of histone $F2A_1$ in: (a) 0.1 *M* NaCl in H_2O–16% D_2O; (b) 0.2 *M* NaCl in H_2O–16% D_2O.

"structured" regions. Histone solutions are known to show some self-aggregation even at concentrations below 1 mg/ml (D. M. J. Lilley, unpublished observation) and hence if the aggregation of these molecules is considered to be a fast process relative to the NMR time scale, and this assumption would appear reasonable in view of the comparatively weak apolar effects involved, then it is apparent that the extent of aggregation at 10 mg/ml is at most 12% of that at 100 mg/ml, and probably less.

The simulation of ^{13}C NMR spectra of 100 mg/ml histone solutions in pure water thus rests on the assumption that aggregation between histone molecules occurs entirely between structured portions of the molecules but this would seem very plausible a priori and is also supported by the evidence of the proton NMR spectra and ^{13}C NMR spectra at lower concentrations.

The general conclusion that histones contain secondary structure when dissolved in pure water is in contrast with views expressed by Bradbury (1972) and Isenberg. D'Anna and Isenberg (1973, 1974a,b) would claim that histones isolated using methods such as those for these studies are denatured in dilute aqueous solution. The addition of salt to this solution produces an increase in α helicity. An important difference between our results and those of Isenberg is that we have never subjected our histones to very high dilutions; in our hands secondary structure appears to have been preserved. It may be important that within the nucleus histone concentrations similar to those used in our studies are present.

It is clear that the conformations of histone molecules which are obtained from simulation of the ^{13}C NMR spectra at 100 mg/ml are really a description of the molecules in terms of hindered and free regions rather than completely random coil and rigorously α-helical regions. In all four histones there are regions designated as being structured which contain proline, and hence cannot be regular α helix. However, in the context of this work structured is taken to mean a region showing a high degree of some kind(s) of secondary structure. For example, a structured region might be composed of short lengths of helix with one or more breaks where the residues at the breaks are still essentially constrained, such that the region behaves as a unit in the aggregation process.

Conclusions

The ^1H NMR and ^{13}C NMR data present a consistent picture of histones as molecules possessing regions of random coil and regions of structure, which are induced to undergo self-aggregation by increases in either ionic strength or protein concentration within the ranges studied here. This is in contrast to the view expressed by Bradbury and Rattle (1972) and D'Anna and Isenberg (1974a,b), where histone molecules are regarded as completely random coil molecules in the absence of salt.

These results allow greater confidence to be placed in the conformations resulting from the simulation method and, furthermore, demonstrate that the concentration induced aggregation processes actually result in a greater sensitivity to conformation of ^{13}C NMR spectra at the higher concentration. These conditions, rather than introducing artefacts into the system, probably are a better representation of the in vivo state of these molecules.

Acknowledgments

We wish to acknowledge the excellent technical support of Mrs. Hazel Briggs and Miss Inger Jönrup. We also wish to thank Bruker Spectrospin for access to their new WH-180 spectrometer and in particular we thank Dr. C. Bradley.

References

Allerhand, A., and Oldfield, E. (1973), *Biochemistry 12*, 3428–3433.

Boublik, M., Bradbury, E. M., and Crane-Robinson, C.

(1970), *Eur. J. Biochem. 14,* 486–497.
Bradbury, E. M., Crane-Robinson, C., Goldman, H., Rattle, H. W. E., and Stevens, R. M. (1967), *J. Mol. Biol. 29,* 507–523.
Bradbury, E. M., and Rattle, H. W. E. (1972), *Eur. J. Biochem. 27,* 270–281.
Clark, V. M., Lilley, D. M. J., Howarth, O. W., Richards, B. M., and Pardon, J. F. (1974), *Nucleic Acids Res. 1,* 865–880.
D'Anna, J. A., and Isenberg, I. (1973), *Biochemistry 12,* 1035–1043.
D'Anna, J. A., and Isenberg, I. (1974a), *Biochemistry 13,* 2093–2098.
D'Anna, J. A., and Isenberg, I. (1974b), *Biochemistry 13,* 2098–2104.
Doddrell, D., Glushko, V., and Allerhand, A. (1972), *J. Chem. Phys. 56,* 3683–3689.
Johns, E. W. (1967a), *Biochem. J. 104,* 78–82.
Johns, E. W. (1967b), *Biochem. J. 105,* 611–614.
Kelley, R. I. (1973), *Biochem. Biophys. Res. Commun. 54,* 1588–1594.
Kornberg, R. D. (1974), *Science 184,* 868–871.
Kornberg, R. D., and Thomas, J. O. (1974), *Science 184,* 865–868.
Li, H. J., Wickett, R. R., and Isenberg, I. (1972), *Biopolymers 11,* 375–397.
Luzzati, V., and Nicolaieff, A. (1963), *J. Mol. Biol. 7,* 142.
McDonald, C. C., and Phillips, W. D. (1969), *J. Am. Chem. Soc. 91,* 1513–1521.
Panyim, S., and Chalkley, R. (1969), *Arch. Biochem. Biophys. 130,* 337–346.
Pardon, J. F., and Richards, B. M. (1973), *Biol. Macromol. 6,* 1–70, 305–322.
Pardon, J. F., and Wilkins, M. H. F. (1972), *J. Mol. Biol. 68,* 115–124.
Prothero, J. W. (1966), *Biophys. J. 6,* 367–370.
Richards, B. M., and Pardon, J. F. (1970), *Exp. Cell Res. 62,* 184–196.
Schiffer, M., and Edmundson, A. B. (1967), *Biophys. J. 7,* 121–135.

An Immunological Approach to the Role of the Low Molecular Weight Subunits in Myosin. I. Physical–Chemical and Immunological Characterization of the Light Chains†

John C. Holt‡ and Susan Lowey*

ABSTRACT: The light chains of chicken breast muscle myosin (alkali 1 and 2, 5,5′-dithiobis(2-nitrobenzoic acid) (DTNB) l.c.) have been isolated in pure form and characterized with respect to amino acid composition, uv and circular dichroism (CD) spectral properties, and molecular weight. Antibodies specific for each of the light chains have been used to demonstrate the similarity of alkali 1 and 2 (mol wt 21,000 and 16,000, respectively), and the distinctness of these from DTNB l.c. (mol wt 18,000). The DTNB l.c. isolated by a variety of methods were all immunologically identical. Significant cross-reactivity was observed between corresponding rabbit and chicken light chains, confirming other indications of homology between these proteins in the two species. The immunological difference between alkali 1 and 2 was largely accounted for by an N-terminal peptide, rich in proline, alanine, and lysine, which is unique to alkali 1. The presence of antibodies to this peptide in anti-alkali 1 serum suggests an immunological approach to the question of how alkali l.c. are distributed in myosin.

All myosins so far studied, whether from vertebrate or invertebrate muscle, or from nonmuscle sources, contain small subunits (mol wt ~20,000) known as light chains (Lowey and Risby, 1971; Sarkar et al., 1971; Lehman et al., 1972; Adelstein and Conti, 1972; Pollard and Korn, 1972). That these are integral components of myosin is implied by their survival of all purification procedures for myosin; moreover, fluorescent antibodies specific for light chains stain only the A-band of myofibrils (Lowey and Steiner, 1972). Since light chains are retained in the proteolytic subfragments heavy meromyosin and subfragment 1, they are presumably localized in or near the globular heads of myosin (Weeds and Lowey, 1971).

As discussed in the following paper (Holt and Lowey, 1975), several lines of evidence suggest that light chains are involved in the hydrolysis of ATP by myosin, although only in the case of invertebrate molluscan myosin is this function understood in any detail. A class of light chain (EDTA l.c.),[1] which can be selectively and reversibly dissociated from scallop myosin, has been shown to be responsible for the myosin-linked Ca-regulation present in this species (Szent-Györgyi et al., 1973). Vertebrate DTNB l.c. can, moreover, substitute for EDTA l.c. in restoring Ca sensitivi-

† From the Rosenstiel Basic Medical Sciences Research Center and the Graduate Department of Biochemistry, Brandeis University, Waltham, Massachusetts 02154. *Received March 25, 1975.* This work was supported by grants from the National Science Foundation (GB 38203), the National Institute of Arthritis, Metabolism and Digestive Diseases, U.S. Public Health Service (AM 17350), and the Muscular Dystrophy Association of America.
‡ Supported by Research Fellowships of the Massachusetts Heart Association (1047-F and 1109-F).

[1] Abbreviations used are: EDTA, ethylenediaminetetraacetic acid; DTNB, 5,5′-dithiobis(2-nitrobenzoic acid); Gdn·HCl, guanidine hydrochloride.